Extended Space Doppler Processing for Non-Cooperative Ground Moving Target Imaging

Samuele Gelli[1,2], Alessio Bacci[1,2], Marco Martorella[1,2], Fabrizio Berizzi[1,2]

[1]University of Pisa, Italy
[2]CNIT-RaSS, Italy

[samuele.gelli,alessio.bacci]@for.unipi.it

ABSTRACT

Non-cooperative moving target appear defocused in SAR image due to the lack of knowledge of the relative motion between radar platform and moving target. The spreading effect induced by uncompensated target motion leads to a low detection capabilities especially in the case of ground moving target where the target returns is lower compared to the clutter return. Moreover in the case of bistatic geometry the problem of clutter non-stationary should be taken into account since this dramatically reduce the detection performance of the conventional STAP filter technique used in monostatic system. In this paper a new bistatic STAP processing operating in space Doppler domain is introduced. The improvement in detection performance make ISAR processing applicable to obtain a well focused image of non-cooperative moving target through the compensation of the relative motion between SAR platform and each detected target.

1. INTRODUCTION

SAR system allows to obtain high cross-range resolution image through the synthetic aperture formation enable by the perfect knowledge between SAR platform and a focus point on the scene. The lack of knowledge between non-cooperative moving target and the platform produce target defocus leading to a blurred and displaced image of any object that is not static during the synthetic aperture formation. ISAR processing allow to view the problem of synthetic aperture formation in another way. In ISAR processing, target motion is crucial in order to obtain high cross-range resolution image and no a-priori information about target motion's is required. Through an appropriate processing chain, ISAR can be used to compensate the unknown part of the relative motion between SAR platform and moving target in order to obtain a well refocused image,[1]. The first step in ISAR refocus processing concern target detection that can be a critical issue especially in the case of small slow ground moving target embedded in strong ground clutter. As know, the coherent processing of the echoes received by different antenna element at different slow-time instant allows to perform clutter filtering in angle/Doppler plane through the Space-Time Adaptive Processing (STAP),[2]. A technique that jointly combine STAP for clutter suppression and ISAR processing for non-cooperative target refocus has been develop in previous works for monostatic system,[3][4]. STAP processing offer superior performance respect to the conventional filtering techniques thanks to the estimation of the clutter covariance matrix that include clutter local spectral characteristic. In optimal STAP the independent and identically distributed (IID) training data hypothesis is typically assumed. Under this hypothesis the estimation of the clutter covariance matrix used in the classical Simple Matrix Inversion (SMI) approach is a maximum likehood estimate (MLE) that asymptotically converge to the exact one as the number of training data increase, [5]. In this case the convergence is only related to the number of training data and not to the interference scenario as each clutter space-time snapshots relative to a particular range cell used in the MLE share the same covariance matrix. Under such consideration, it is also possible to observe that the IID condition on training data is equivalent to the homogeneous clutter environment assumption. However, IID assumption is very restrictive and is violated is some real scenario. Typically two

factor affects the stationary of training data: clutter heterogeneity and range dependence of clutter angle/Doppler trajectories caused by movements of the transmitter and receiver platform. For the first case, temporally and spatially varying clutter environment, weather phenomenon, clutter edges and other type of clutter heterogeneity, cause an alteration in the STAP covariance matrix estimation that lead to a degradation in detection performance, [6]. In general, it is possible to observe that clutter returns exhibit a Doppler shift that vary with the platform velocity as well as the direction and the width of the antenna beam,[7]. In this case, the acquisition geometry play an important role because influence clutter angle/Doppler response at given range cell and more generally clutter angle/Doppler behaviour can show some degrees of variation along range dimension due to the geometry effects. Range dependence, that appear most severe in multichannle bistatic configurations, strongly degrades STAP performance leading to a mismatch between estimate and exact covariance matrix. In order to restore STAP detection performance under non-stationary clutter environment, a new version of STAP derived from multichannel range-Doppler algorithm used in ISAR processing is developed. The proposed algorithm termed Extended Space Doppler Adaptive Processing (ESDAP), is based on Space Doppler Adaptive Processing (SDAP) algorithm, previously developed in [3], and exploit a first order Taylor series expansion of the SDAP weight vector to take into account linear variation of clutter Doppler frequency. As well as SDAP, also the proposed algorithm perform both clutter suppression and platform motion compensation leading to a defocused image of moving target. ESDAP-ISAR is then proposed to obtain high resolution image of non-cooperative moving target after detection. In Section 2 signal model for bistatic geometry and the Space Doppler Adaptive Processing is briefly examined in order to described, in Section 3, its extended version. Finally results on simulated data and conclusion are presented in Section 4 and Section 5, respectively.

2. SIGNAL MODEL AND MONOSTATIC CLUTTER SUPPRESSION

2.1. BISTATIC MULTICHANNEL SIGNAL MODEL

Let consider the case in which a bistatic system observes a moving target. The receiver employ a phased array of P channels. After range compression, the received signal for the generic $p-th$ channel, $p=1,\ldots,P$, can be expressed in the frequency/slow-time domain as:

$$S_p(f,t)=S_{p,t}(f,t)+S_{p\,c}(f,t)+N_p(f,t) \tag{1.1}$$

where $f\in\left[f_0-\frac{B}{2},f\ +\!\!-\right.$ and $t\in\left[-\frac{obs}{2},\frac{T_{obs}}{2}\right]$. The received signal can be seen as a sum of three contributions in which the first term represent the target contribution, the second is the contribution due to the static scene, denoted in this case as clutter, and the last is the additive Gaussian noise term. The formulation can be easily extended to a discretized version in which $S_p(n,m)=S_p(n\Delta f,mT_R)$:

$$S_p(n,m)=S_{p,t}(n,m)+S_{p\,c}(n,m)+N_p(n,m) \tag{1.2}$$

where the n and m index represents the discrete frequency index and the transmitted pulse respectively, while T_R is the pulse repetition frequency. The first two contributions, reported in eq.(1.2), can be expressed as, [3]:

$$S_{p,t}(n,m)=e^{-j\frac{4\pi}{}R_{B,t}(m)}\sum_{i=1}^{N_s}\sigma_i e^{-j\frac{\pi}{\lambda}\left[K_t(m)\left(y^{(\ )}\Omega_{eff\ Bi}mT_R+x^{(i)}\right)\right.} \tag{1.3}$$

$$S_{p,c}(n,m) = e^{-j\frac{4\pi}{}R_{B\,c}(m)} \iint_{x,y} \sigma(x,y) e^{-j\frac{\pi}{\lambda}\left[K_c(m)\left(y\Omega_{eff,Bc}mT_R+x\right)\right.} dxdy \tag{1.4}$$

In these equations $(x^{(\,)}, y^{(i)})$ represent the coordinate of the generic scatter, $R_{B,t}$ represent the bistatically equivalent monostatic radar-target distance, $\Omega_{eff,Bt}$ is the bistatic effective rotation vector produced by the relative motion between receiver and target while K_t is the distortion term introduced by bistatic geometry that depends on the bistatic angle between transmitter, receiver and a reference point on the target and σ_i is the amplitude of the $i-th$ scatter. The same quantities can be defined for the signal received by the static scene, i.e. clutter, with the only difference that all quantities are exactly known. To better define the signal model for the scenario under consideration, a statistical model of the bistatic clutter is needed. The authors previously developed in [8] a model based on the autocorrelation function that take into account clutter range dependence.

2.2. HETEROGENEITY AND GEOMETRY EFFECTS ON CLUTTER MODEL

In the case of IID assumption it is easy to demonstrate that the estimated clutter covariance matrix, that is crucial in order to obtain the STAP filter weigh vector, is not related to the interference scenario. This condition is equivalent to a homogeneous clutter environment assumption. For a correct estimation of the covariance matrix a large number of training data along range dimension is required and this is equivalent to have a large area of stationary clutter. For this reason, the IID assumption is very restrictive and is violated in some real scenario. For example, due to the motion of the objects within the observed clutter cell (e.g. tree and other vegetation) pulse-to-pulse decorrelation of the received clutter can produce an alteration in the STAP covariance matrix estimation. This effect, termed Internal Clutter Motion (ICM), [9], is typically expressed in the form of covariance matrix taper, [10] and cause an increase of the covariance matrix rank deteriorating STAP filter performance. In conclusion all the various type of clutter heterogeneity, possibly combined with the effect due to the use of a bistatic geometry, breach the classical IID assumption used in SMI approach and lead to a mismatch between estimate and exact covariance matrices. In Fig. 1, an example of clutter heterogeneity as consequence of ICM effects is reported in angle/Doppler plane for different wind conditions. The spectral model of the clutter is obtained by a series of measurements performed by MIT Lincoln Lab, [11]. In this figure, the Doppler shift of the stationary clutter seen by the radar varies with the desired look angle due to the motion of the platform resulting in a well know two-dimensional "ridge" in angle/Doppler space. Pulse-to-pulse decorrelation is quite evident. In order to show clutter range dependence that produce a strongly degradation of STAP performance, clutter angle/Doppler trajectories for four different range cells relative to a bistatic multichannel geometry (Fig. 3) are reported in Fig. 2. This result is obtained from simulation performed by Warsaw University of Technology.

2.3. SPACE DOPPLER ADAPTIVE PROCESSING

High resolution image can be obtained by applying the range-Doppler algorithm:

$$F_{D,p}(n,m_v) = DFT_m\left\{S_{p,t}(n,m)S^*_{p,ref}(n,m)\right\} \tag{1.5}$$

where DFT is the discretized Fourier transform along the slow-time dimension, m_v represent the Doppler frequency index and $S_{p,ref}(n,m) = e^{-j\frac{4\pi}{\lambda}R_{B,0}(m)}$ is the reference signal that take into account only the relative motion between platform and static point on the ground. Eq.(1.5) can be seen as a discrete convolution between the receive signal and reference signal both expressed in frequency/Doppler frequency domain:

$$F_{D,p}(n,m_v) = S_{p,t}(n,m_v) \otimes_{m_v} S_{p,ref}(n,-m_v) \tag{1.6}$$

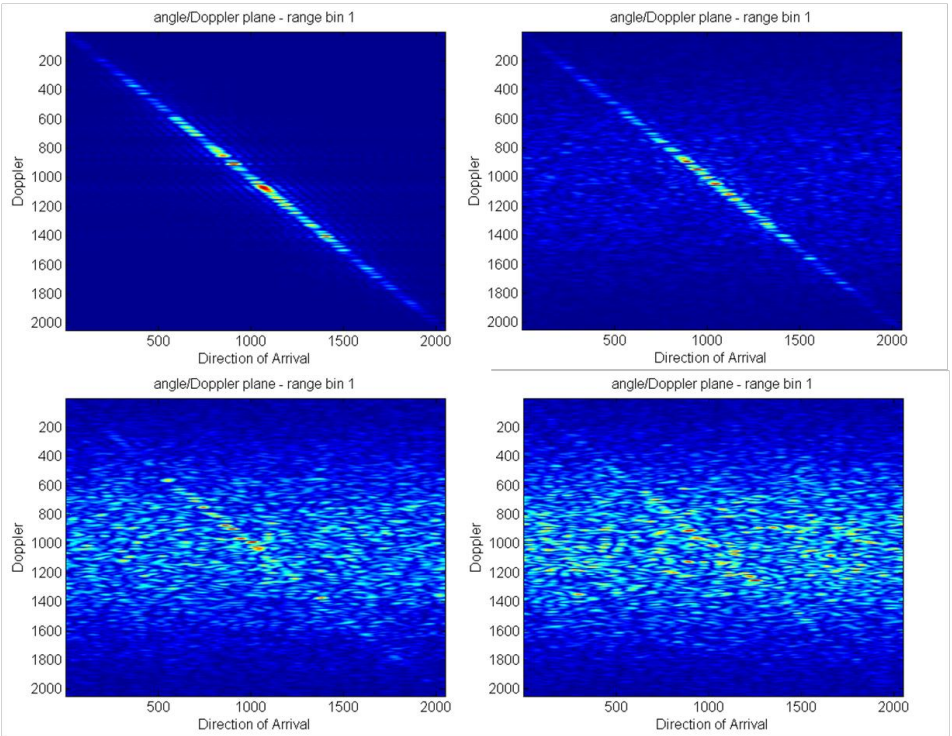

Fig. 1 Clutter behaviour in angle/Doppler plane in heterogeneous clutter due to ICM effects for different wind conditions

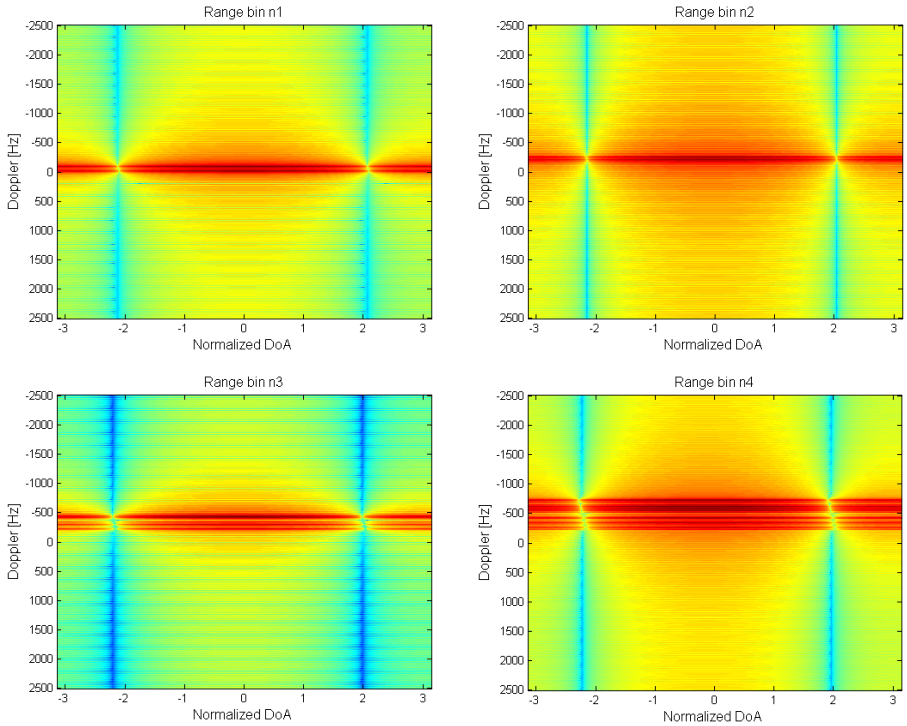

Fig. 2 Clutter angle/Doppler trajectories for multichannel bistatic geometry

As it is possible to see, the range-Doppler image formation algorithm can be seen as a matched filter (MF) in the frequency-Doppler domain. MF operation can be easily extended for a multichannel scenario and can be expressed in a vectorial form through a staking operation implemented first along channel dimension and after along Doppler dimension, as:

$$F_{D,p}(n,m_v) = \mathbf{G}^H(n,m_v)\ \ (n) \tag{1.7}$$

$$\begin{aligned} \mathbf{S}(n,m_v) &= \left[S_1(n,m_v), S_2(n,m_v), \ldots, S_P(n,m_v)\right]^T \quad \mathbb{C}^{P\times 1} \\ \mathbf{S}_{ref}(n,m_v) &= \left[S_{1,ref}(n,m_v), S_{2,ref}(n,m_v), \ldots, S_{P,ref}(n,m_v)\right]^T \quad \mathbb{C}^{P\times 1} \end{aligned} \tag{1.8}$$

$$\begin{aligned} \mathbf{S}(n) &= \left[\mathbf{S}(n,0)^T, \mathbf{S}(n,1)\ , \ldots, \mathbf{S}(n,M-1)\right]^T \quad \mathbb{C}^{MP\times 1} \\ \mathbf{G}(n\ m_v) &= \left[\mathbf{S}_{ref}(n,m_v)\ , \mathbf{S}_{ref}(n,m_v-1)^T, \ldots, \mathbf{S}_{ref}(n,m_v\quad (M-1))^T\right]^T \in \mathbb{C}^{MP\times 1} \end{aligned} \tag{1.9}$$

where M is the Doppler frequency bin. Optimal Space-Doppler Adaptive Processing (SDAP) replace the reference vector with the optimal weigh vector in SINR sense:

$$F_{D,p}(n,m_v) = \mathbf{W}^H(n,m_v)\ \ (n) \tag{1.10}$$

$$\mathbf{W}(n,m_v) = \gamma\ \hat{}\ {}_D^{-1}\mathbf{G}(n,m_v) \tag{1.11}$$

The scaling constant will not affect the SINR, while the estimation of cross power spectral matrix can be obtained with a set of N_r target free training data in the space-Doppler domain:

$$\hat{\mathbf{R}}_D = \frac{1}{N_r}\sum_{n_r=0}^{N_r-1}\mathbf{Z}(n\ )\mathbf{Z}^H(\ _r) \in \mathbb{C}^{MP\times MP} \tag{1.12}$$

It is worth to pointing out that this formulation is different for post-Doppler STAP in [2] because of the space-Doppler definition of the reference vector. To obtain a well focused image of moving target, the reference vector must take into account both platform and target motion. This is a unrealistic situation such as target is non-cooperative and in the real case reference vector perform only platform motion compensation. The relative motion between platform and target is compensated through the use of ISAR processing.

3. EXTENDED SPACE DOPPLER PROCESSING

A possible way to take into account clutter Doppler frequency variation along range dimension consists in exploiting a power series expansion of the instantaneous weight vector. Extended Space Doppler Adaptive Processing technique is proposed. ESDAP processing employed a truncated Taylor series of the weight vector retaining only constant and linear terms. This technique does not require any prior information about bistatic geometry but it uses only the information received by the array with the cost of doubling the Degrees of Freedom (DoFs) and, as consequence, the computational burden. Assuming to consider only linear variation on time, the weight vector can be modelled as the sum of a fixed component and a component varying linearly with time:

$$\mathbf{W}(n_r,m)=\mathbf{W}_0(n_r,m)+n_r\Delta\mathbf{W}(n_r,m) \tag{1.13}$$

where n_r is the range cell index that is related to the range position r by the relation $r=n_r\Delta_r$ where $\Delta_r=\dfrac{c}{2B\cos\beta}$ is the bistatic range resolution. In order to avoid range cell migration a filtering operation in the frequency domain is performed leading to the discrete frequency/slow-time domain:

$$(n,m)=DFT_r\{\mathbf{W}(n_r,m)\} \tag{1.14}$$

As in previous section, it is possible to perform ESDAP first by considering the DFT along slow-time dimension:

$$\mathbf{W}(n,m_v)=DFT_m\{\quad(n,m)\} \tag{1.15}$$

Then the beamformer output can be expressed as:

$$\begin{aligned}F_{ESDAP}(n,m_v)&=\mathbf{W}_0{}^H(n,m_v)\mathbf{S}(n)+n_r\Delta\mathbf{W}\quad(n,m_v)\mathbf{S}(n)=\\&=\mathbf{W}'^H(n,m_v)\mathbf{T}^H{}_{n_r}\mathbf{S}(n)\quad\mathbf{W}'^H(n,m_v)\mathbf{S}'(n)\end{aligned} \tag{1.16}$$

where $\mathbf{T}_r=[\mathbf{I},\ {}_r\mathbf{I}]\in C^{MP\times 2MP}$ and $\mathbf{I}\in\mathbb{C}^{MP\times MP}$ is the identity matrix while $\mathbf{W}'^H(n,m_v)$ is the new doubled weight vector expressed as $\mathbf{W}'(n,m_v)\quad\begin{bmatrix}\mathbf{W}_0(n,m_v)\\ \Delta\mathbf{W}(n,m_v)\end{bmatrix}\in C^{\ MP\times 1}$. By using the same MVDR constraints, as in monostatic STAP case, it is possible to obtain a solution for $\mathbf{W}'(n,m_v)$:

$$\mathbf{W}'(n,m_v)=\gamma'\hat{\mathbf{R}}^{-1}_{esdap}\mathbf{G}'(n,m_v)\quad C^{2MP\times 1} \tag{1.17}$$

where $\mathbf{G}'(n,m_v)\quad\begin{bmatrix}\mathbf{G}(n,m_v)\\ 0\end{bmatrix}\in C^{\ MP\times 1}$ in which $\mathbf{G}(n,m_v)$ has been defined in previous section. The estimation of new cross-power spectral matrix can be obtained by considering a suitable set of N_r target free training data in space-Doppler domain $\mathbf{Z}'(n_r)=\begin{bmatrix}\mathbf{Z}(n_r)\\ n_r\mathbf{Z}(n\end{bmatrix}$ where $\mathbf{Z}(n_r)$ has been defined in section 2.3:

$$\hat{\mathbf{R}}'_{esdap}=\frac{1}{N_r}\sum_{n_r=1}^{N_r-1}\mathbf{Z}'(n_r)\mathbf{Z}'^H(n_r)\quad C^{2MP\times 2MP} \tag{1.18}$$

This new covariance matrix can be simply written as:

$$\hat{\mathbf{R}}'_{esdap}\quad\begin{bmatrix}\hat{\mathbf{R}}^{(0)} & {}^{(1)}_{D}\\ \hat{\mathbf{R}}^{(1)}_{D} & {}^{(2)}_{D}\end{bmatrix}\in C^{2MP\times 2MP} \tag{1.19}$$

where each single matrix $MP\times MP$ can be expressed as:

$$\hat{\mathbf{R}}_D^{(k)} = \frac{1}{N_r}\sum_{n_r=1}^{N_r-1} n_r{}^k \mathbf{Z}(n_r)\mathbf{Z}^H(n_r) \quad C^{MP\times MP} \tag{1.20}$$

It is worth pointing out that the number of training range cells to obtain an average loss of between adaptive and optimal implementation (also known as RMB rules) cannot be available. It is quite evident that this case a sub optimum approach to overcome these problems is needed.

4. RESULTS AND CONSIDERATIONS

To demonstrate the effectiveness of the proposed ESDAP-ISAR processing, a dataset simulated by Warsaw University of Technology, Institute of Electronic Systems, has been used. The terrain has been modelled by using a digital elevation model (DEM) with a dimension of $500m \times 500m$. Two slow moving targets are present in the scene, in particular a large trailer truck with a radial velocity of $10m/s$ and a military truck with a radial velocity of $5m/s$. A point-like slow moving target with a radial velocity of $3m/s$ has been also added in the image to better demonstrate the detection capabilities of the proposed processing. Two different type of bistatic geometry has been simulated. In the first case both transmitter and receiver fight at the same speed and in parallel direction, as its possible to see from Fig. 3. In the second case, transmitter and receiver flight paths are orthogonal. This configuration is more complex respect to the first case because the configuration change with time as do the Doppler characteristics. The geometry for this case is represented in **Errore. L'origine riferimento non è stata trovata.** while the system parameters for both geometry are reported in Table 1 and Table 2 respectively.

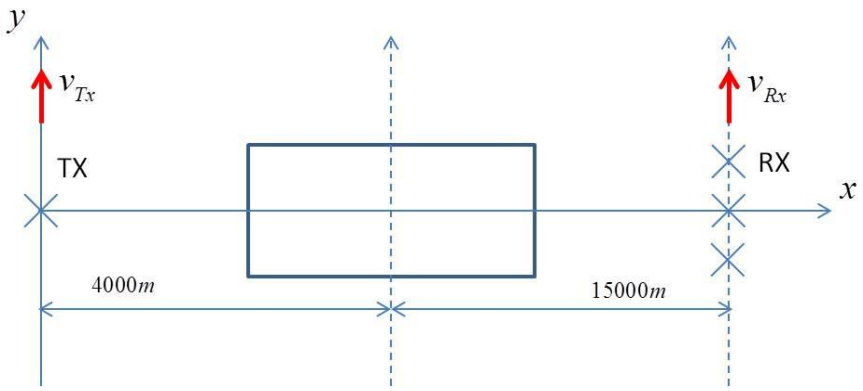

Fig. 3 Bistatic multichannel geometry at t=0: Case 1

4.1. RESULTS FOR BISTATIC GEOMETRY 1

In this subsection results of the ESDAP processing applied to the first bistatic geometry, are shown. In Fig. 5 are respectively represented the original range-Doppler image of the scene and the result obtained by applying monostatic SDAP processing. As it is possible to see by a visual inspection, all moving targets are not visible neither in the range-Doppler SAR image and nor in the image obtained after SDAP processing due to the non-stationary clutter environment. Fig. 6a) shows the result obtained by applying ESDAP processing. As its possible to see clutter suppression seem to work good as all the slow moving targets become visible. To better appreciate the difference of the approaches, a comparison between slices obtained by the bidimensional null filtering in the angle/Doppler domain show that ESDAP processing can suppress only zero-Doppler clutter region allow to detect slow moving targets (see Fig. 6b)). After detection, it is possible to crop each detected target in order to isolate it from the other target and static scene contribution. A well focused image of moving target can be obtained by applying ISAR processing to each crop. In Fig. 7 and Fig. 8 is reported the images before and after ISAR processing. The

improvement in the image focus is evident.

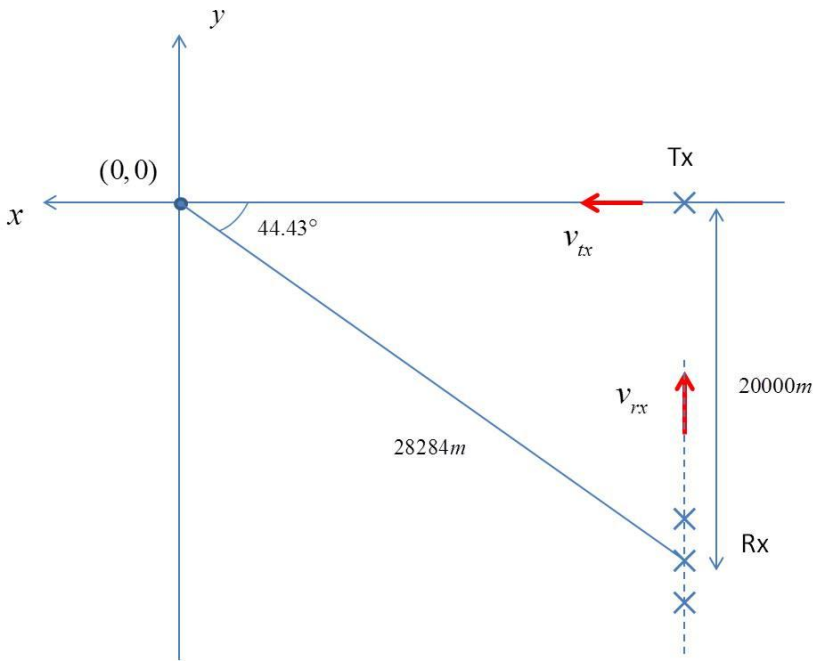

Fig. 4 Bistatic multichannel geometry at t=0: Case 2

Tx Parameters

Look Angle	45°
Platform Velocity	50 m/s
f_0 (central frequency)	9.6 GHz
Altitude	4000 m
Tx Bandwidth	500 MHz
PRF	5 KHz
ADC Sampling Rate	25 MHz
Observation Time	0.4 s

Rx Parameters

Look Angle	73.3°
Platform Velocity	50 m/s
ADC Sampling Rate	25 MHz
Altitude	4500 m

Observation Time	0.4 s

Table 1 Transmitter and receiver systems parameters for geometry 1

Tx Parameters

Look Angle	78.69°
Platform Velocity	50 m/s
f_0 (central frequency)	9.6 GHz
Altitude	4000 m
Tx Bandwidth	500 MHz
PRF	5 KHz
ADC Sampling Rate	25 MHz
Observation Time	0.4 s

Rx Parameters

Look Angle	81.95°
Platform Velocity	60 m/s
ADC Sampling Rate	25 MHz
Altitude	4000 m
Observation Time	0.4 s

Table 2 Transmitter and receiver parameters for geometry 2

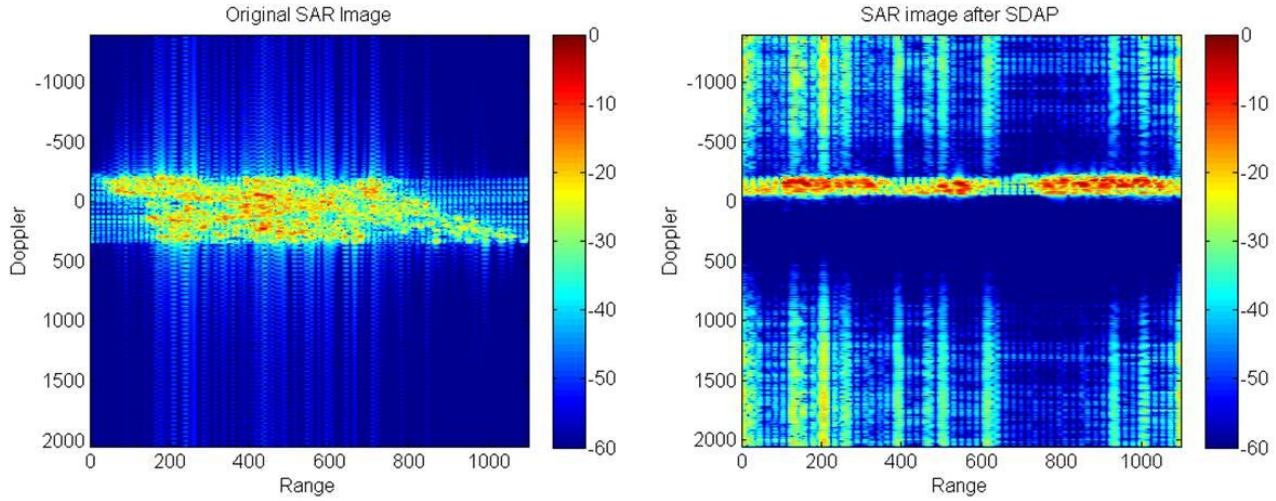

Fig. 5 Range Doppler SAR image. a)SAR image of the scene. b)Image after SDAP processing

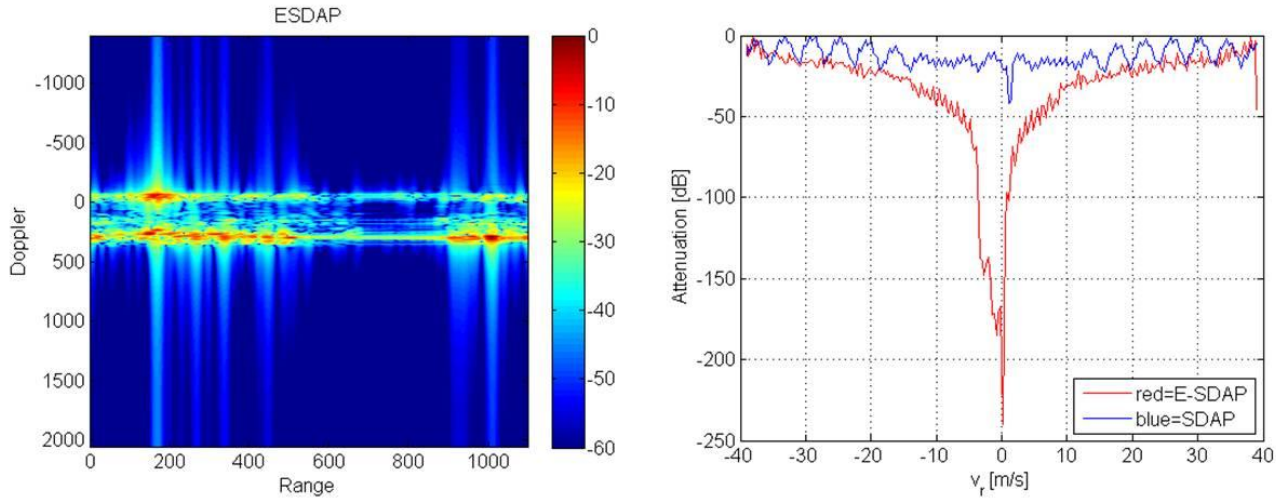

Fig. 6 a)Range Doppler SAR image after ESDAP processing. b)Comparison between SDAP and ESDAP null filters

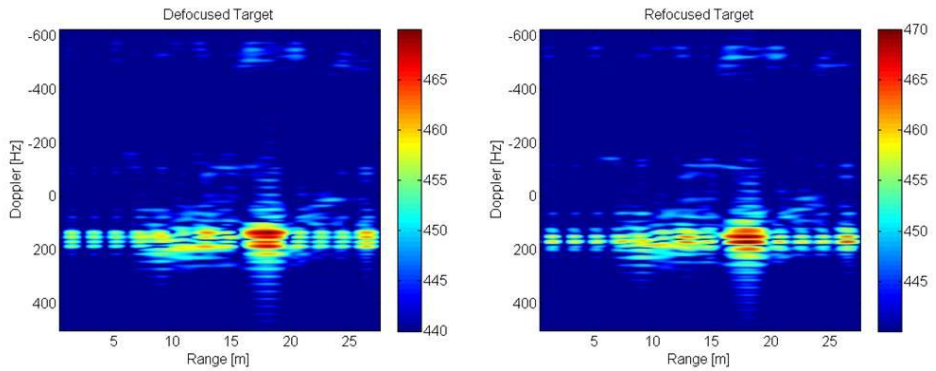

Fig. 7 Refocus ISAR image. a)Crop1. b)Refocused crop

4.2. RESULTS FOR BISTATIC GEOMETRY 2

In this subsection results of ESDAP processing applied to the second bistatic scenario are shown. As in previous case, Fig. 9 represent range-Doppler SAR image and range-Doppler image after the SDAP processing, respectively. Also for this case slow moving targets are not visible in neither image. Fig. 10a)

show the result obtained by applying ESDAP processing. As its possible to see clutter suppression seem to work good also for this bistatic configuration. In Fig. 10b) a comparison between SDAP and ESDAP null filters show again that the proposed approach can suppress only clutter region differently than monostatic SDAP. ISAR processing is applied to the SAR image crops to obtain well focused image of targets. Results are show in Fig. 11, Fig. 12 and Fig. 13respectively.

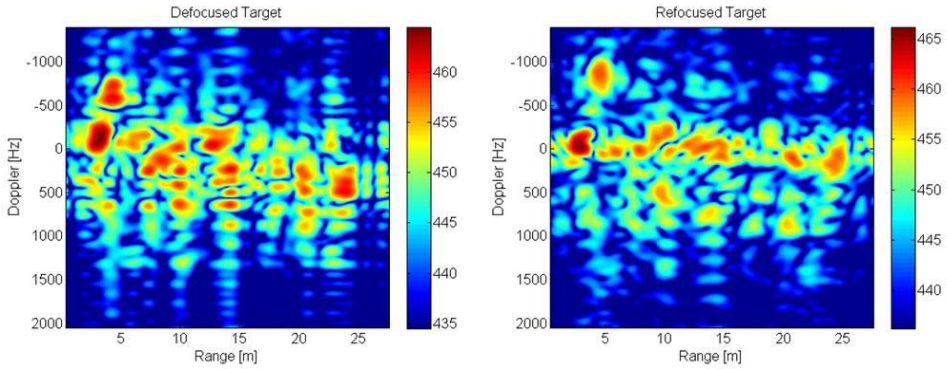

Fig. 8 Refocus ISAR image. a)Crop2. b)Refocused crop

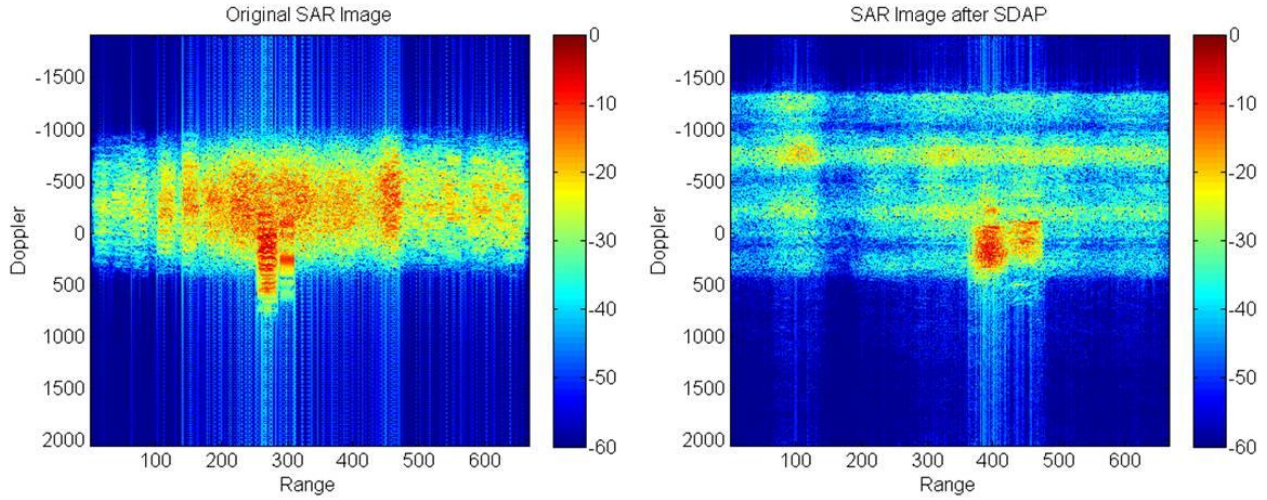

Fig. 9 Range Doppler SAR image. a)SAR image of the scene. b)Image after SDAP processing

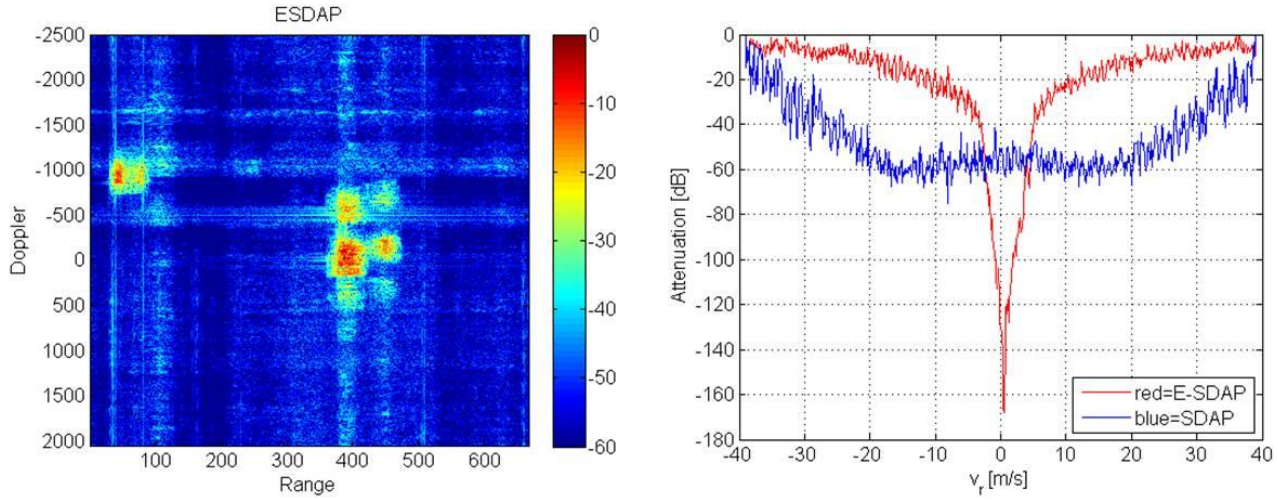

Fig. 10 a)Range Doppler image after ESDAP processing. b)Comparison between SDAP and ESPAP null filters

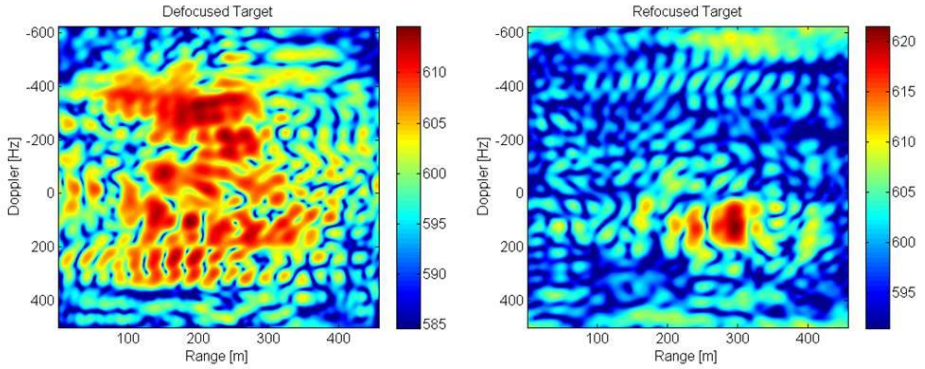

Fig. 11 Refocus ISAR image. a)Crop1. b)Refocused crop

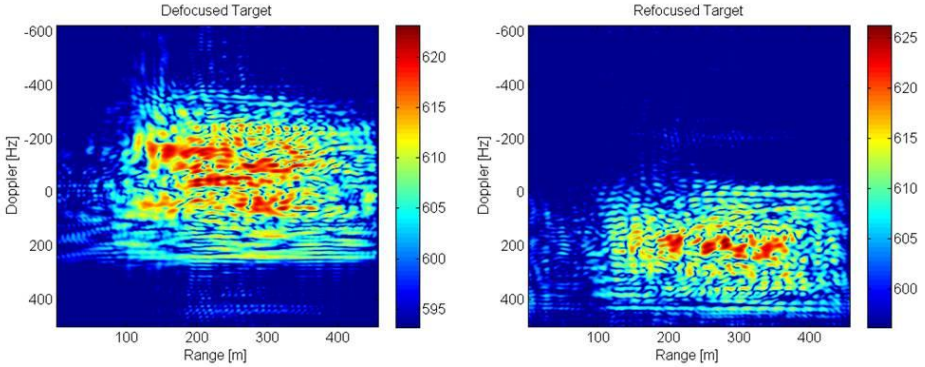

Fig. 12 Refocus ISAR image. a)Crop2. b)Refocused crop

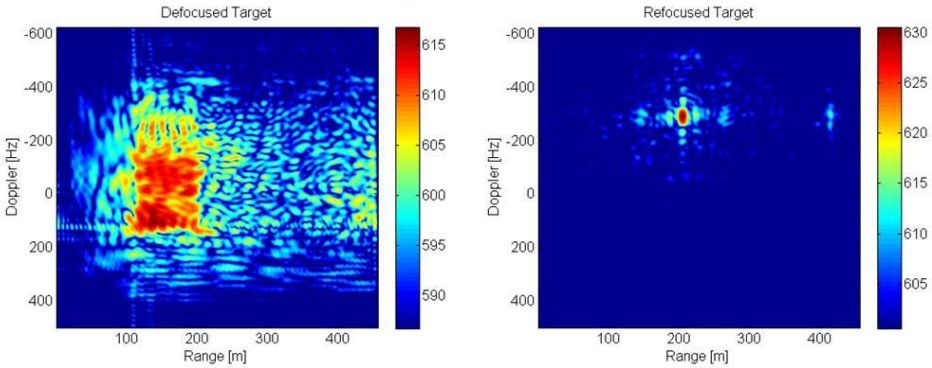

Fig. 13 Refocus ISAR image. a)Crop3. b)Refocused crop

5. CONCLUSION

The applicability of ESDAP-ISAR processing has been demonstrated on simulated data for two different bistatic multichannel geometry. The proposed processing offer better detection performance compared to monostatic SDAP processing.

REFERENCES

[1] M. Martorella, E. Giusti, F. Berizzi, A. Bacci and E. D. Mese, "ISAR based techniques for refocusing non-cooperative targets in SAR images," in *IET Radar, Sonar & Navigation*, vol. 6, no. 5, pp. 332-340, June 2012. doi: 10.1049/iet-rsn.2011.0310

[2] W. L. Melvin, "A STAP overview," in *IEEE Aerospace and Electronic Systems Magazine*, vol. 19, no. 1, pp. 19-35, Jan.

2004.

[3] A. Bacci, M. Martorella, D. A. Gray and F. Berizzi, "Space-Doppler adaptive processing for radar imaging of moving targets masked by ground clutter," in *IET Radar, Sonar & Navigation*, vol. 9, no. 6, pp. 712-726, 7 2015.

[4] A. Bacci, D. Gray, M. Martorella and F. Berizzi, "Joint STAP-ISAR for non-cooperative target imaging in strong clutter," *2013 IEEE Radar Conference (RadarCon13)*, Ottawa, ON, 2013, pp. 1-5.

[5] I. S. Reed, J. D. Mallett and L. E. Brennan, "Rapid Convergence Rate in Adaptive Arrays," in *IEEE Transactions on Aerospace and Electronic Systems*, vol. AES-10, no. 6, pp. 853-863, Nov. 1974.

[6] W. L. Melvin, "Space-time adaptive radar performance in heterogeneous clutter," in *IEEE Transactions on Aerospace and Electronic Systems*, vol. 36, no. 2, pp. 621-633, Apr 2000.

[7] R. Klemm, "Comparison between monostatic and bistatic antenna configurations for STAP," in *IEEE Transactions on Aerospace and Electronic Systems*, vol. 36, no. 2, pp. 596-608, Apr 2000.

[8] S. Gelli, A. Bacci, M. Martorella and F. Berizzi, "A sub-optimal approach for bistatic joint STAP-ISAR," *2015 IEEE Radar Conference (RadarCon)*, Arlington, VA, 2015, pp. 0992-0997.

[9] P. M. Techau, J. S. Bergin and J. R. Guerci, "Effects of internal clutter motion on STAP in a heterogeneous environment," *Radar Conference, 2001. Proceedings of the 2001 IEEE*, Atlanta, GA, 2001, pp. 204-209.

[10] J. R. Guerci, "Theory and application of covariance matrix tapers for robust adaptive beamforming," in *IEEE Transactions on Signal Processing*, vol. 47, no. 4, pp. 977-985, Apr 1999.

[11] P. Lombardo and J. B. Billingsley, "A new model for the Doppler spectrum of windblown radar ground clutter," *Radar Conference, 1999. The Record of the 1999 IEEE*, Waltham, MA, 1999, pp. 142-147.